Aus der Universitätsklinik für Kardiologie, Inselspital Bern

Direktor: Prof. Dr. med. Stephan Windecker

Arbeit unter der Leitung von Prof. Dr. Dr. med. Christoph Gräni

Reproducibility of 4D cardiac computed tomography feature tracking myocardial strain and comparison against speckle-tracking echocardiography in patients with severe aortic stenosis

Inaugural-Dissertation zur Erlangung der Doktorwürde der Humanmedizin

der Medizinischen Fakultät der Universität Bern

vorgelegt von

Grogg-Trachsel Hanna

von Frutigen BE

publiziert im Journal of Cardiovascular Computed Tomography

Von der Medizinischen Fakultät der Universität Bern auf Antrag der Dissertationskommission als Dissertation genehmigt.

_____

Promotionsdatum:

Der Dekan der Medizinischen Fakultät:

Journal of Cardiovascular Computed Tomography xxx (xxxx) xxx

Contents lists available at ScienceDirect

Journal of Cardiovascular Computed Tomography

journal homepage: www.JournalofCardiovascularCT.com

Research paper

Reproducibility of 4D cardiac computed tomography feature tracking myocardial strain and comparison against speckle-tracking echocardiography in patients with severe aortic stenosis

Benedikt Bernhard [a], Hanna Grogg [a], Jan Zurkirchen [a], Caglayan Demirel [a], Daniel Hagemeyer [a], Taishi Okuno [a], Nicolas Brugger [a], Stefano De Marchi [a], Adrian T. Huber [b], Martina Boscolo Berto [a], Giancarlo Spano [a], Stefan Stortecky [a], Stephan Windecker [a], Thomas Pilgrim [a], Christoph Gräni [a,*]

[a] Department of Cardiology, Inselspital, Bern University Hospital, University of Bern, Switzerland
[b] Department of Diagnostic, Interventional and Paediatric Radiology, Inselspital, Bern University Hospital, University of Bern, Bern, Switzerland

ARTICLE INFO

Keywords:
4D cardiac computed tomography
Feature tracking
Speckle-tracking echocardiography
Myocardial strain
Deformation imaging
Global longitudinal strain

ABSTRACT

Background: Myocardial strain is an established parameter for the assessment of cardiac function and routinely derived from speckle tracking echocardiography (STE). Novel post-processing tools allow deformation imaging also by 4D cardiac computed tomography angiography (CCT). This retrospective study aims to analyze the reproducibility of CCT strain and compare it to that of STE.

Methods: Left (LV) and right ventricular (RV), and left atrial (LA) ejection fraction (EF), dimensions, global longitudinal (GLS), circumferential (GCS) and radial strain (GRS) were determined by STE and CCT feature tracking in consecutive patients with severe aortic stenosis evaluated for transcatheter aortic valve implantation.

Results: 106 patients (mean age 79.9 ± 7.8, 44.3% females) underwent CCT at a median of 3 days (IQR 0–28 days) after STE. In CCT, strain measures showed good to excellent reproducibility (intra- and inter-reader intraclass correlation coefficient ≥0.75) consistently in the LV, RV and LA. In STE, only LV GLS and LA GLS yielded good reproducibility, whereas LV GCS and LV GRS showed moderate, and RV GLS and free wall longitudinal strain (FWLS) poor reproducibility. Agreement between CCT and STE was strong for LV GLS only, while other strain features displayed moderate (LV GCS, LA GLS) or weak (LV GRS, RV GLS and FWLS) inter-modality correlation.

Conclusion: LV, RV and LA CCT strain assessments were highly reproducible. While a strong agreement to STE was found for LV GLS, inter-modality correlation was moderate or weak for LV GCS, LV GRS, and RV and LA longitudinal strain, possibly related to poor reproducibility of STE measurements.

1. Introduction

Endo- and myocardial strain are established determinants in the evaluation of myocardial contractility,[1] describing the degree of deformation of cardiac walls within the cardiac cycle. Deformation of a cardiac cavity can occur along its long axis (global longitudinal strain – GLS), its perimeter (global circumferential strain – GCS), or by thickening of its wall (global radial strain – GRS).[2] A large body of evidence supports the high diagnostic and prognostic value of left ventricular (LV) GLS,[3] while results for LV GCS and GRS are inconclusive.[4–6] GLS mainly mirrors the contractility of subendocardial longitudinal fibers that often display impaired function in the early phase of myocardial injury, when LV ejection fraction (LVEF) can still be maintained.[7] LV GLS provides incremental value beyond LVEF in the prediction of adverse events in patients with chronic heart failure,[8,9] ischemic heart disease,[10] myocarditis,[11] valvular heart disease,[12–15] and several other cardiac diseases.[4,16–18]

Speckle-tracking echocardiography (STE) uses unique interference patterns ("speckles") that are followed across the cardiac cycle to obtain the degree of deformation and derive strain. Speckles result from the naturally occurring inhomogeneous reflection of acoustic signals in the myocardium due to the different orientation of muscle fibers and are displayed in varying grayscales in B-mode echocardiography. More recently, the introduction of novel post-processing tools enable feature tracking (FT) based strain evaluation also by 4D cardiac computed

* Corresponding author. Director Cardiovascular Imaging Department of Cardiology University Hospital Bern, Freiburgstrasse CH, 3010, Bern, Switzerland.
E-mail address: christoph.graeni@insel.ch (C. Gräni).

https://doi.org/10.1016/j.jcct.2022.01.003
Received 26 October 2021; Received in revised form 20 January 2022; Accepted 22 January 2022
Available online xxxx

Please cite this article as: Bernhard B, Grogg H, Zurkirchen J, Reproducibility of 4D cardiac computed tomography feature tracking myocardial strain and comparison against speckle-tracking echocardiography in patients with severe aortic stenosis, Journal of Cardiovascular Computed Tomography, https://doi.org/10.1016/j.jcct.2022.01.003

Abbreviations

CCT	4-dimensional cardiac computed tomography
CMR	cardiac magnet resonance
CV	chamber view
EDA/EDV	end diastolic area/volume
EF	ejection fraction
ESV	end systolic volume
FAC	fractional area change
FT	feature tracking
FWLS	free wall longitudinal strain
GCS	global circumferential strain
GLS	global longitudinal strain
GRS	global radial strain
ICC	intraclass correlation coefficient
LA	left atrium
LV/RV	left/right ventricle
SAX	short axis
STE	speckle tracking echocardiography
TAVI	transcatheter aortic valve implantation

tomography angiography (CCT). FT is an algorithm-based approach, identifying and tracking characteristic features of endo- and epicardial borders.[19] In addition to image characteristics (brightness, greyscale), also anatomic landmarks are taken into account to assess strain.[20] Broad evidence that supports the clinical value of this promising tool derived from CCT in a real-world setting is widely lacking. Although CCT involves ionized radiation, it might be beneficial in selected patients and can overcome limitations of STE such as poor acoustic window and foreshortening of the ventricles due to suboptimal probe position dictated by the patient's anatomy. Moreover, 4D CCT acquisition protocols are recommended standard in several clinical settings, such as planning of transcathether aortic valve implantation (TAVI)[21] and extracting all available information from these clinically indicated CCT examinations is warranted. The present study aims to determine the reproducibility of CCT strain compared to STE in the left (LV) and right ventricle (RV), and the left atrium (LA).

2. Methods

2.1. Study cohort

Between October 2019 and March 2021, consecutive patients with severe aortic stenosis evaluated for TAVI at Bern University Hospital, Switzerland were enrolled in an institutional registry, which is part of the SwissTAVI registry (NCT01368250). Inclusion criteria for the present study were the conduction of a complete CCT scan (0–100% of RR interval with 5% increments reconstructions and 20 phases) and transthoracic echocardiography at our institution prior TAVI. Patients unable to provide written consent were excluded. The study was approved by the local ethics committee and was conducted in accordance with the Declaration of Helsinki.

2.2. Image acquisition and measurements

Clinically indicated retrospectively ECG-gated CCT imaging was performed using a dual-source 128-row multisclice CT (Somaton Definition Flash; Siemens Healthcare, Erlangen, Germany) as previously described.[22] Scan parameters were as following: reference tube voltage was set to 100–120 kv and reference tube-current-time product 300 mAs_{ref} according to the body weight; rotation time 0.28 s; slice collimation 128 × 0.6 mm; pitch value 0.17 for spiral acquisition 0–100% of the RR interval. Automatic current modulation (CareDose4D) was used for raw data acquisition. Each patient received an intravenous injection of 40–120 ml of contrast medium at a flow rate of 4–5 ml/s depending on body-weight. Image acquisition was performed during an inspiratory breath-hold in a cranio-caudal direction and images were reconstructed in 1 mm increment using an I30f kernel (SAFIRE, strength 3). CCT datasets in 5% increments were reconstructed throughout the entire cardiac cycle, resulting in 20 reconstructions per scan (0–100%). STE was performed during clinical routine on machines of different vendors by investigators with varying experience following a standardized protocol[23] that, among others, included a short axis stack (SAX) of the LV, overview as well as LV- and RV focused depictions in the apical 4-chamber view (CV), LA-focused apical 2-CV and LV-focused apical 2- and 3-CV.

Both CCT and STE images underwent standardized analysis on dedicated workstations by investigators blinded to the clinical information and findings of the other imaging modality (i.e. authors HG for CCT, JZ for STE, and BB for reproducibility analysis). Echocardiographic images were analyzed by speckle-tracking using TOMTEC Arena 2D cardiac performance analysis, (TOMTEC Imaging Systems GmBH, Unterschleissheim, Germany), whereas Medis Suite v.3.0, (Medis Medical Imaging, Leiden, The Netherlands) was used for segmentation (Medis Suite 3D Viewer) and strain-analysis (Medis Suite QStrain) of CCT images. Both applications use semi-automatic tools to trace endo- and epicardial borders in each view in endsystole and enddiastole. Endo- and epicardial tracings were manually checked for accuracy in each frame throughout the entire cardiac cycle and manually revised by the investigator if required. Prior to analysis, readers rated the quality of the images they considered most suitable for strain analysis on a scale from 1 to 4.1 – poor (e.g. severe arrhythmia or breathing artefact), 2 – moderate (e.g. challenging blood pool-endocardium delineation in all frames), 3 – good (e.g. lack of optimal epicardium soft-tissue delineation in parts in selected frames), 4 – excellent (no limitations). LV GLS was averaged from apical 2-, 3- and 4-CV after tracing of endocardial borders with exclusion of papillary muscles (Fig. 1). For CCT images, the reader previously reformatted 2-, 3- and 4-CV and a SAX stack. LV GCS and GRS were assessed in 3 SAX slices (at the height of the mitral valve, the papillary muscles and the apex). RV and LA strain and dimensions were determined monoplane in the 4- and 2-CV, respectively. For the LA contours the pulmonary veins and the left atrial appendage were excluded (Fig. 1). LA GLS (equivalent to LA reservoir strain) was defined as the peak of the LA strain curve compared to ventricular enddiastole as baseline. LV dimensions and LVEF were calculated by Simpson's biplane method in both STE and CCT.

STE and CCT datasets of 15 randomly selected patients underwent additional analysis, (including multiplanar reconstruction for CCT) by the same and an additional reader blinded to previous findings in order to assess reproducibility.

2.3. Statistical analysis

Statistical analysis was conducted with IBM SPSS Statistics 25 (IBM Corp., Armon, New York, USA). Results are presented as mean ± standard deviation or as frequencies and percentage if appropriate. Non-normally distributed variables were provided as median and interquartile range (IQR). Reproducibility of measures was evaluated by intraclass correlation coefficient (ICC), determined with a two-way random effects model for intra- and interreader variability in 15 patients. Intraclass correlation was interpreted according to Koo et al. (ICC ≥0.9 – excellent, ICC = 0.75–0.89 – good, ICC = 0.5–0.74 – moderate, ICC<0.5 – poor).[24] Agreement between CCT and STE was visualized in Bland-Altman plots with determination of the mean bias between modalities. Upper and lower limits of agreement (LOA) were defined as mean bias ± 1.96 x standard deviation. Bivariate Pearson correlation was used to describe correlation between CCT and STE measurements and interpreted according to Schober et al. (r ≥ 0.9 – very strong correlation, r = 0.7–0.89 – strong, 0.4–0.7 –moderate, r = 0.1–0.39 – weak).[25] Mean relative disagreement was calculated as ratio between the mean of both measurements (CCT and STE) and the differences between

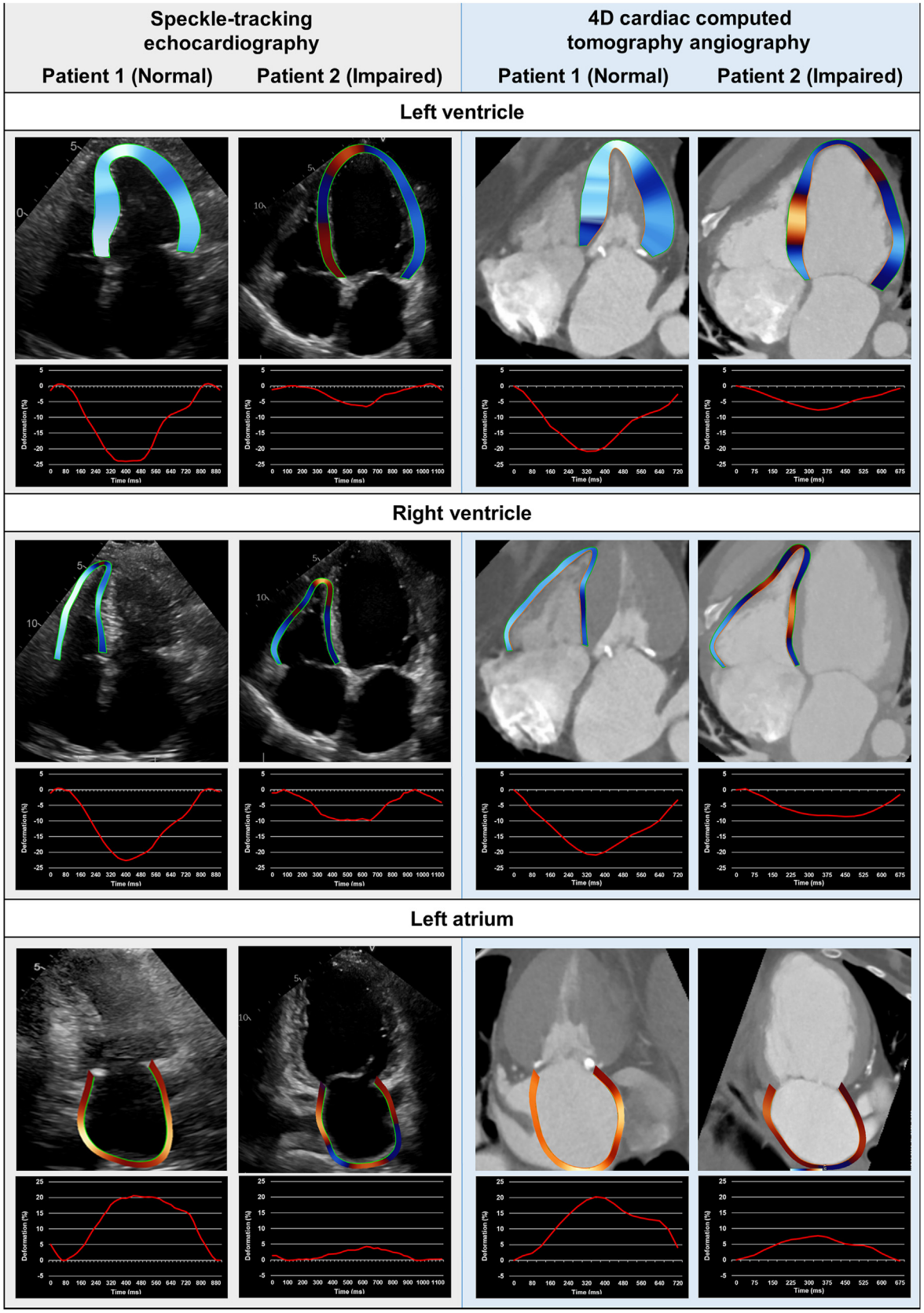

Fig. 1. Global longitudinal strain (GLS) in endsystolic frames of a patient with normal (*patient 1*) and highly impaired (*patient 2)* left- and right ventricular and left atrial function. Positive and negative strain values are denoted in red and blue color, respectively. Dark and bright colors represents a low and a high degree of deformation, respectively. (For interpretation of the references to color in this figure legend, the reader is referred to the Web version of this article.)

both measurements. Mean disagreement across groups stratified by image quality and time delay between STE and CCT were compared by unpaired t-tests or by Mann-Whitney *U* test.

3. Results

Among 310 consecutive patients with severe aortic stenosis referred for the evaluation of TAVI, 106 patients were included in the present study (Fig. 2) of whom 91 (86%) underwent TAVI after CCT and STE imaging. Another n = 7 patients were referred to surgical aortic valve replacement and n = 8 patients were not deemed eligible for TAVI. Mean age was 79.9 ± 7.8 years and 59 (56%) were male (Table 1). Median time delay between CCT and STE was +3 days (IQR 0–28 days). For the complete CCT including CT angiography of the thorax and potential TAVI vascular access sites, patients received 85.5 ± 14.3 ml (median 90 ml) contrast agent and the median total dose-length product was 957 (IQR 680 to 1179) mGycm. Image quality (IQ) was rated as excellent in 66 (62.3%) of patients (34% good, 2.8% moderate and 0.9% poor) in CCT and in 10 (9.4%) patients (38.7% good, 36.8% moderate, 15.1% poor) in STE. STE apical views were available in 104 (98%), SAX in 88 (83%), RV in 94 (88%) and LA in 104 (98%) of patients. STE loops were assessed with 51.3 ± 7.9 frames per second and a mean heart rate of 73.2 ± 13.4 bpm. Mean heart rate in CCT was 69.8 ± 13.7 bpm, resulting in a mean temporal resolution of 23.6 ± 4.9 frames per second. No patient was excluded due to poor image quality.

3.1. Reproducibility

In CCT, all measurements showed good (ICC >0.75–0.9) to excellent (ICC >0.9) intra- and interreader variability (Table 2 *and* ***Graphic Abstract***). All CCT derived LV apical measurements (LV EDV, LV EF, LV GLS), and LA EDV as well as LA EF showed both excellent intra- and interreader variability. In STE, only LA ESV yielded excellent reproducibility, while LV apical measurements (LV EDV, LV EF, LV GLS) and LA GLS were still well reproducible. However, short axis (LV GCS and LV GRS) and RV measurements were of moderate or poor robustness. RV GLS and RV free wall longitudinal strain (FWLS) were not significantly correlated across readers in STE.

3.2. Agreement of CCT and STE

We observed relevant discrepancies between most CCT and STE measurements (for absolute values see Supplemental Table S1). Only LV apical measurements (LV EDV, LV EF, and LV GLS) showed good agreement and strong correlation, but also considerable limits of agreement (LOA) (Fig. 3). Mean LV GLS was −13.2 ± 5.3% in CCT and −16.0 ± 5.4% in STE, resulting in a mean inter-modality bias of 2.79% (LOA 9.1 to −3.6%). LVEF was 48.8 ± 17% in CCT and 51.6 ± 13.6% in STE (mean bias −2.88%; LOA -25.2 to 19.5%). CCT slightly underestimated both variables (less negative values for LV GLS, lower values for LVEF), while LV EDV was consistently overestimated (mean bias + 68.7 ml (LOA -11.5 to 149.9 ml) in CCT compared to STE. SAX measurements (LV GRS and LV GCS) showed wide LOAs and moderate (GCS) or poor (GRS) correlation between both modalities. Consistent with the poor reproducibility in STE, STE RV measurements did not correlate to them of CCT, except for moderate correlation of RV EDA (Fig. 4). LA GLS, as well as LA ESV

Table 1
Patient characteristics.

	Total (n = 106)
Age (years)	79.9 ± 7.8
Gender (female)	47 (44%)
Body-Surface-Area (m^2)	1.87 ± 0.25
Body-Mass-index (kg/m^2)	27.5 ± 5.9
NYHA class II or III	100 (94%)
STS PROM score	4.8 ± 4.46
History of CAD	58 (54.7%)
History of prior myocardial infarction	13 (12.3%)
Arterial hypertension	95 (89.6%)
Atrial fibrillation	27 (25.5%)
Diabetes mellitus	24 (22.6%)
Permanent pacemaker	8 (7.5%)
Implantable Cardioverter Defibrillator	4 (3.8%)
LV mass (g)	224.7 ± 72
LV mass index (g/m^2)	120.5 ± 36.8
LVEDV (ml)	114 ± 54
LVEF (%)	51.6 ± 13.6
SV (ml)	55.1 ± 19.2
SV index	29.6 ± 9.7
AVA (cm^2)	0.87 ± 0.3
AV mean gradient (mmHg)	31.7 ± 15.7
AV peak gradient (mmHg)	52.3 ± 24
LV end-diastolic pressure (mmHg)	14.4 ± 12.3
Hemoglobin (g/l)	12.2 ± 1.9
Creatinine (μmol/l)	122.8 ± 62.2

Abbreviations: AVA – aortic valve area, CAD – coronary artery disease, EF – ejection fraction, LV – Left ventricular, NYHA – New York Heart Association, STS PROM-predicted risk of mortality according to the Society of Thoracic Surgeons Risk Score, SV - stroke volume.

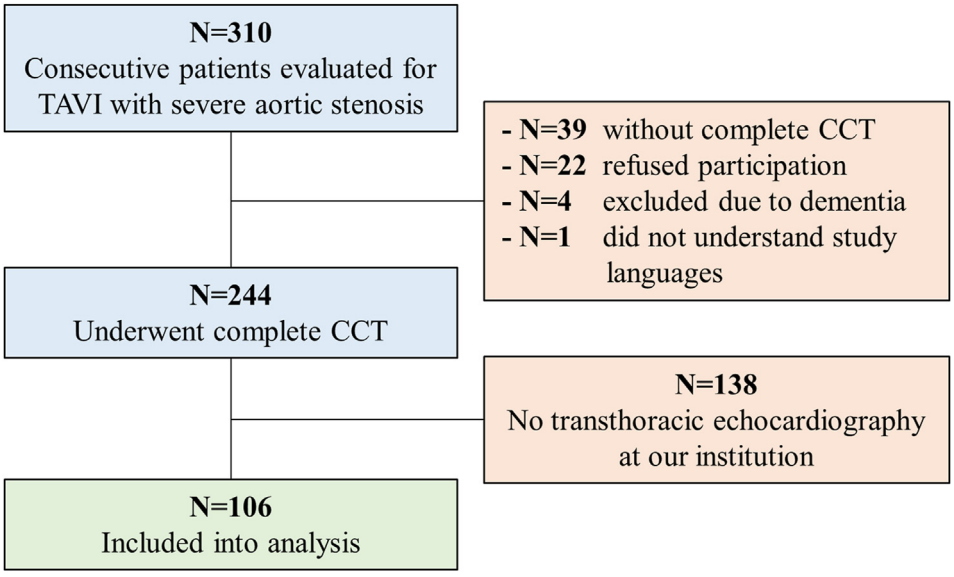

Fig. 2. Study consort flow chart. Abbreviations: CCT – 4D cardiac computed tomography, TAVI – transcatheter aortic valve implantation.

Table 2
Reproducibility (intraclass correlation coefficient (ICC) and 95% CI) of CCT and STE measurements.

		Left ventricle					Right ventricle				Left atrium		
		EDV	EF	GLS	GCS	GRS	EDA	FAC	GLS	FWLS	ESV	EF	GLS
CCT	Intra-Reader N=15	**0.993** 0.979 to 0.998 p<0.001	**0.965** 0.898 to 0.988 p<0.001	**0.949** 0.854 to 0.982 p<0.001	**0.940** 0.831 to 0.979 p<0.001	**0.807** 0.517 to 0.931 p<0.001	**0.887** 0.696 to 0.960 p<0.001	**0.920** 0.780 to 0.973 p<0.001	**0.880** 0.681 to 0.958 p<0.001	**0.877** 0.674 to 0.957 p<0.001	**0.937** 0.822 to 0.978 p<0.001	**0.965** 0.899 to 0.988 p<0.001	**0.916** 0.770 to 0.971 p<0.001
	Inter-Reader N=15	**0.980** 0.942 to 0.993 p<0.001	**0.975** 0.927 to 0.991 p<0.001	**0.960** 0.887 to 0.987 p<0.001	**0.928** 0.801 to 0.975 p<0.001	**0.888** 0.700 to 0.961 p<0.001	**0.798** 0.499 to 0.927 p<0.001	**0.808** 0.519 to 0.931 p<0.001	**0.753** 0.409 to 0.910 p<0.001	**0.835** 0.578 to 0.941 p<0.001	**0.985** 0.955 to 0.995 p<0.001	**0.962** 0.891 to 0.987 p<0.001	**0.896** 0.719 to 0.837 p<0.001
STE	Intra-Reader N=15	**0.895** 0.718 to 0.964 p<0.001	**0.865** 0.646 to 0.953 p<0.001	**0.944** 0.843 to 0.981 p<0.001	**0.615** 0.170 to 0.852 p=0.006	**0.511** 0.019 to 0.804 p=0.021	**0.797** 0.497 to 0.927 p<0.001	**0.718** 0.342 to 0.895 p=0.001	**0.210** -0.11 to 0.321 p=0.782	**0.431** -0.84 to 0.765 p=0.058	**0.916** 0.769 to 0.869 p<0.001	**0.839** 0.586 to 0.943 p<0.001	**0.799** 0.5 to 0.928 p<0.001
	Inter-Reader N=15	**0.871** 0.660 to 0.955 p<0.001	**0.839** 0.585 to 0.943 p<0.001	**0.830** 0.567 to 0.940 p<0.001	**0.622** 0.18 to 0.855 p=0.005	**0.549** 0.07 to 0.822 p=0.014	**0.698** 0.308 to 0.887 p=0.001	**0.611** 0.163 to 0.850 p=0.006	**0.100** -0.413 to 1.066 p=0.453	**0.189** -0.281 to 0.428 p=0.628	**0.841** 0.590 to 0.742 p<0.001	**0.725** 0.355 to 0.898 p=0.001	**0.814** 0.532 to 0.934 p<0.001

Interpretation of ICC	
Excellent	≥0.9
Good	0.75-0.89
Moderate	0.5-0.74
Poor	<0.5

Intraclass correlation coefficients were interpreted according to Koo et al.[24]
Abbreviations: CCT – Cardiac computed tomography, EDV/A – end diastolic volume/area, EF – ejection fraction, ESV/A – end systolic volume/area, FAC – fractional area change, FWLS – free wall longitudinal strain, GCS – global circumferential strain, GLS – global longitudinal strain, GRS – global radial strain, ICC – intraclass correlation coefficients, STE – speckle tracking echocardiography.

and LA EF moderately correlated between modalities but exhibited wide LOAs (Fig. 5).

3.3. Impact of image quality

To investigate whether poor agreement was related to image quality (IQ), we determined the mean relative deviation ("mean relative error") from the average value of both modalities to allow for a comparison of measurements with different units (Fig. 6). Lowest mean relative deviation was found for LV EF (20.5%) and LV GLS (27.1%) and highest for LV GRS (84.8%) and RV GLS (71.2%). Excluding patients with moderate or poor image quality in STE was associated with a significant reduction in the mean relative deviation of LV GLS ($p = 0.003$), LV GRS ($p = 0.01$), RV EDA ($p < 0.001$), RV FWLS ($p = 0.026$), LA ESV ($p = 0.001$), and LA EF ($p = 0.008$) (Supplemental Table S1). No improvement was seen after exclusion of patients with poor or moderate IQ ($n = 4$) in CCT and a time delay between STE and CCT >1 day ($n = 70$).

4. Discussion

In the present study, we compared myocardial strain in CCT against STE in patients with severe aortic stenosis. The findings can be summarized as follows: a) 4D CCT provides images of high quality that allow assessment not only of LV and LA, but also of RV feature tracking strain with high reproducibility; b) using STE, only LV GLS and LA GLS were reproducible and c) agreement of CCT to STE was strong for LV GLS only, but can be increased if STE images of poor quality are excluded.

Lower reproducibility of STE derived LV GCS and GRS in comparison to GLS was already reported by other studies.[26–28] In addition to poor image quality in the short axis view – particularly in the apical segments, also lower lateral resolution of echocardiography can contribute to poor reproducibility.[29] 2D STE requires the speckles to move in parallel direction to the ultrasound lines on that specific image plane which enables a better tracking in the apical views compared to the SAX.[30] Moreover, the echocardiographic acquisition of an appropriate SAX and the post-processing for GCS and GRS assessments requires higher expertise, if compared to GLS derived from the long axis views.[27] Nevertheless, other studies reported higher reproducibility of STE LV strain acquisition compared to the results in our cohort.[26,31,32] In contrast to our analysis, these studies systematically excluded patients with poor image quality (7–25% of patients), which might contribute to this inconsistency.

STE RV and LA strain were less reproducible than STE LV strain in our study. Both, RV and LA strain were derived from a single slice, whereas LV strains were averaged from 3 SAX (base, papillary muscle, apex) or 3 apical slices (2-, 3- and 4CV), respectively. Hence, RV and LA acquisitions are more susceptible to foreshortening and imaging artefacts. The assessment of RV GLS requires complete depiction of the RV from base to the apex and clear delineation of the endocardium from the blood pool. Both can be complicated by the limited echocardiographic accessibility of the RV due to its proximity to the sternum and the complex right ventricular geometry with thin and trabeculated walls that are difficult to delineate from soft tissue.[33] The significantly lower volume estimates (RV EDA) in STE compared to CCT also suggest that full visualization of the RV cavity was not consistently achieved in STE, potentially contributing to poor reproducibility. None of these limitations exists in CCT and the present study demonstrated that RV strain can be assessed with high reproducibility by CCT FT.

Most strain features had a relevant inter-modality bias in our study. Not surprisingly, agreement between STE and CCT was highest in parameters with good reproducibility in both modalities (dimensional LV and LA measurements, LVEF and LV- and LA GLS) and limited for LV SAX- (LV GCS and GRS) and RV measurements. Correlation between modalities improved after exclusion of patients with poor or moderate IQ in STE. Accuracy of STE strain is highly dependent from the acoustic window and IQ, and similar findings were reported from a study comparing CMR and STE.[32] CCT consistently overestimated volumetric variables (LV EDV, RV EDA and LA ESV) and underestimated (resulting in less negative values) LV- and LA GLS compared to STE. Previous studies, comparing both modalities also reported an underestimation of LV- and LA GLS in CCT but described a higher agreement between modalities compared to our findings.[28,34–37] However, these studies systematically excluded a large number of patients with poor IQ in STE (up to about 50%

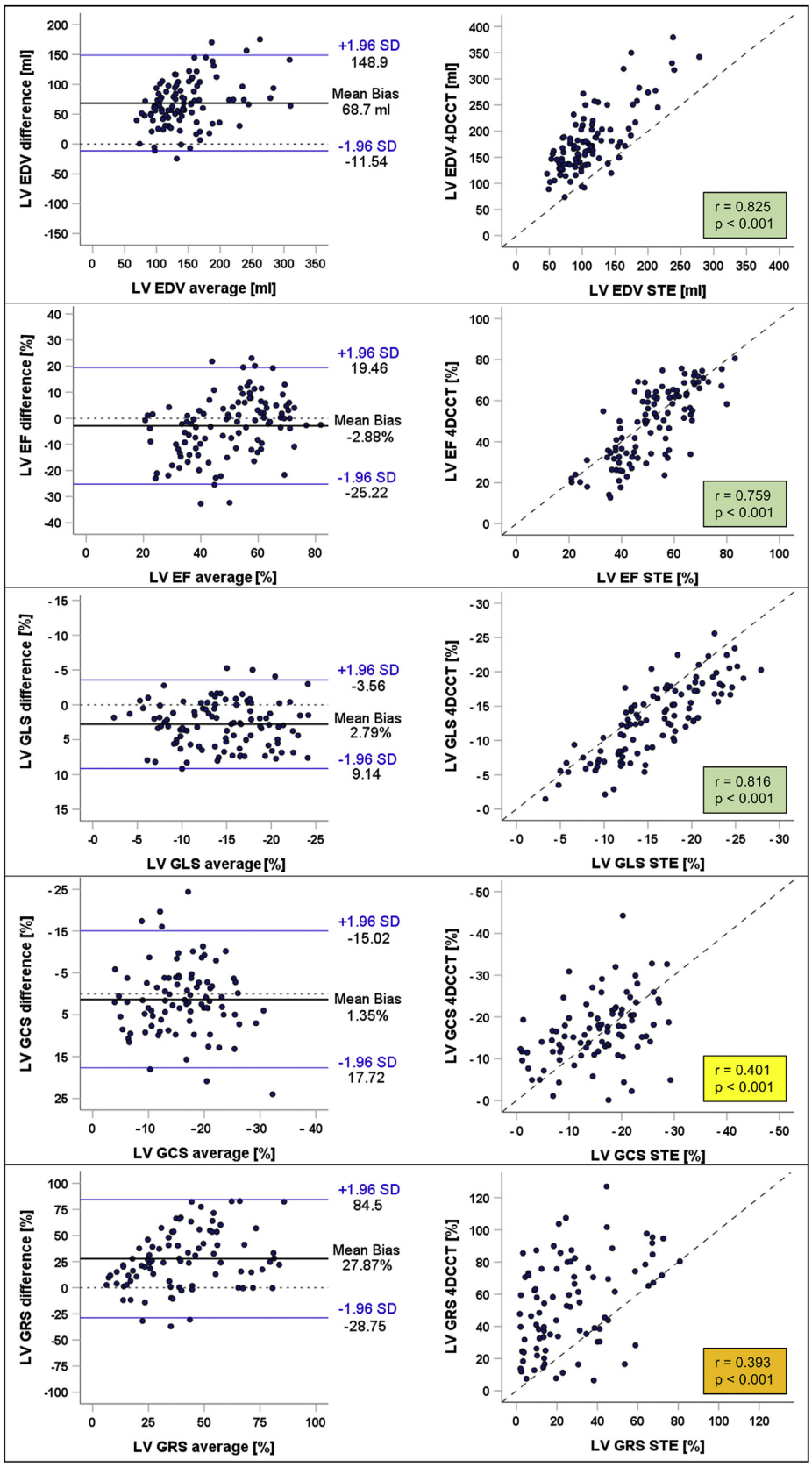

Fig. 3. Agreement and correlation of CCT and STE measurements in the LV. Correlation coefficients were interpreted according to Schober et al.[25] Abbreviations: CCT – 4D cardiac computed tomography, EDV – end diastolic volume, EF – ejection fraction, GCS – global circumferential strain, GLS – global longitudinal strain, GRS – global radial strain, LV – left ventricle, SD – standard deviation, STE – speckle tracking echocardiography.

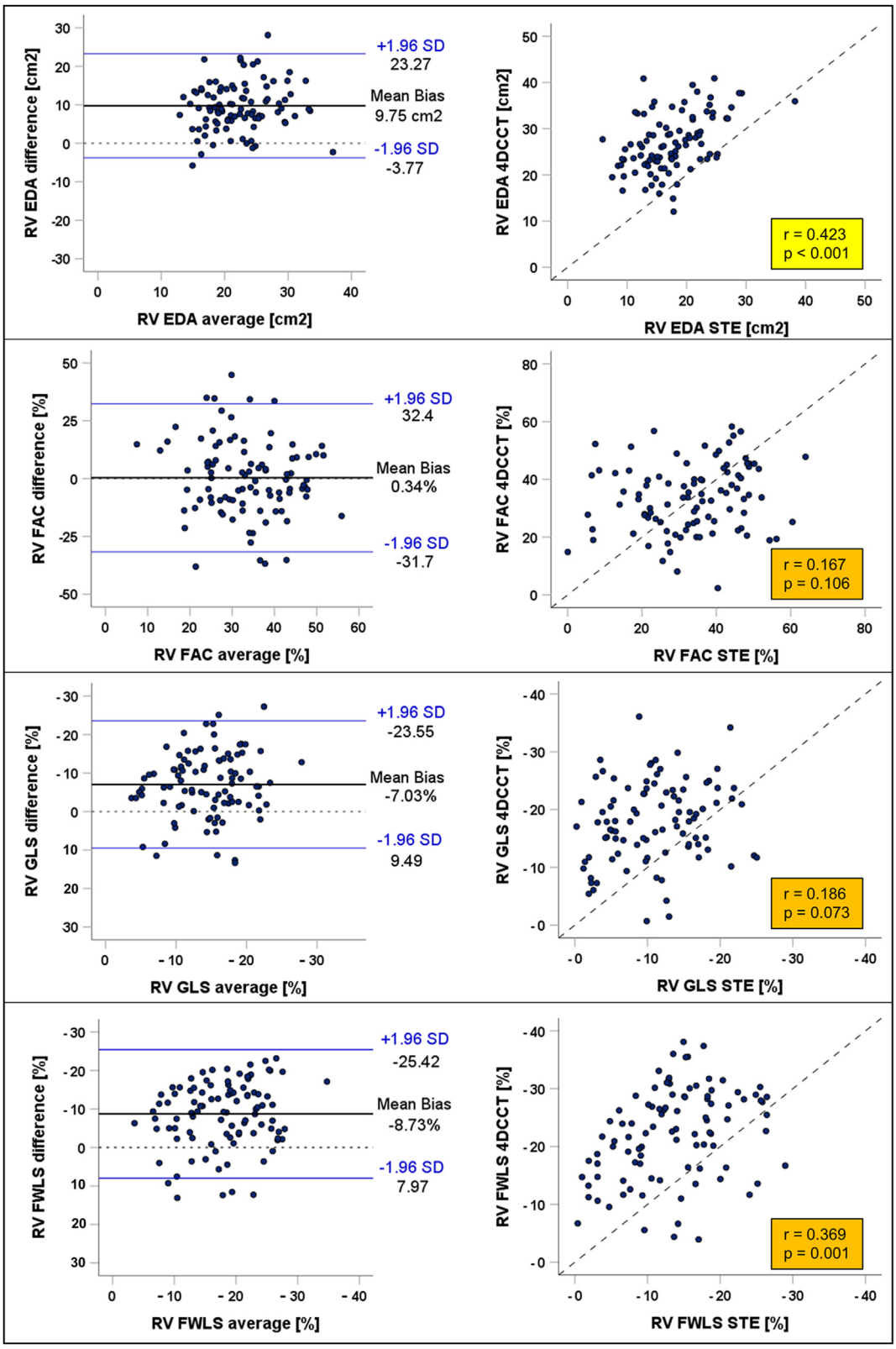

Fig. 4. Agreement and correlation of CCT and STE measurements in the RV. Correlation coefficients were interpreted according to Schober et al.[25] Abbreviations: CCT – 4D cardiac computed tomography, EDA – end diastolic area, FAC – fractional area change, FWLS – free wall longitudinal strain, GLS – global longitudinal strain, RV – right ventricle, SD – standard deviation, STE – speckle tracking echocardiography.

of patients) and, besides Buss et al.,[28] increments of every 10% of the cardiac cycle were rendered, resulting in only 10 reconstructions per cardiac cycle. We hypothesize that, similar to CMR,[38,39] also the lower temporal resolution of CCT compared to STE contributes to inter-modality bias, since maximal deformation (peak strain) is less likely to be captured in sequences with a lower number of frames. Also in our

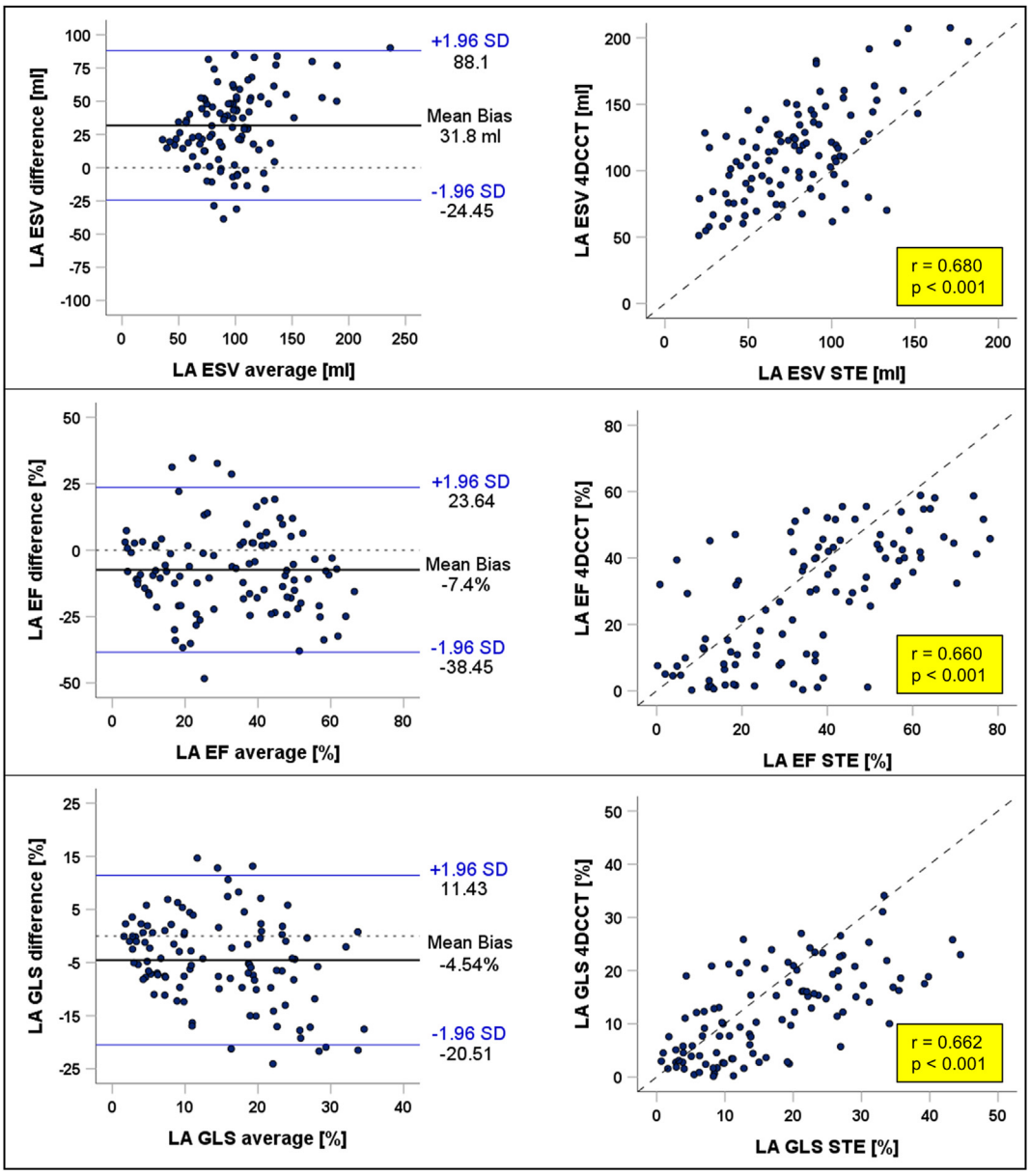

Fig. 5. Agreement and correlation of CCT and STE measurements in the LA. Correlation coefficients were interpreted according to Schober et al.[25] Abbreviations: CCT – 4D cardiac computed tomography, EDV – end diastolic volume, EF – ejection fraction, GLS – global longitudinal strain, LA – left atrium, SD – standard deviation, STE – speckle tracking echocardiography.

study, the number of frames varied between CCT (20 reconstructions (5%) in each RR-interval) and STE (mean 43.4 ± 9.8 frames in each RR-interval).

These results demonstrate that strain values derived from STE and CCT are not interchangeable and separate cut-off values have to be considered to implement CCT strain to clinical practice. Despite a systematic underestimation, clinical interpretation (but not cut-off values) might be similar for CCT longitudinal strain and two studies demonstrated the value of CCT LV GLS in the prediction of mortality in patients undergoing TAVI.[40,41] Another study comparing LV strain assessed by CCT, CMR tagging and STE reported higher correlations of CMR to CCT versus CMR to STE, pointing to a high validity of CCT strain.[42] However, despite its limitations, STE will remain the standard modality to determine strain, but CCT can be a valuable adjunct in patients with clinically indicated CCT or impaired acoustic window in STE. Whereas this study could proof the reproducibility of CCT strain acquisition in the LV, the LA, and for the first time also in the RV, the diagnostic accuracy of RV strain has to be validated against CMR strain imaging in future trials. In addition to LV strain, the assessment of RV and LA might offer the potential to more adequately predict outcomes and tailor management in patients that undergo interventions in which these variables might be interest, such as transcatheter interventions on the mitral- and tricuspid valve.

5. Limitations

Limitations are based on the nature of this retrospective observational study. STE and CCT were not consistently performed at the same day, which might contribute to an underestimation of the correlation of strain measures between modalities. However, in comparison to other cardiac disease like acute myocardial infarction, myocarditis, or takotsubo cardiomyopathy, severe aortic stenosis can be considered to be a mostly stable disease with slow progression and changes in cardiac contractility over time. Changes in ventricular loading conditions over time can also impact strain values,[43] but in our analysis we found no difference

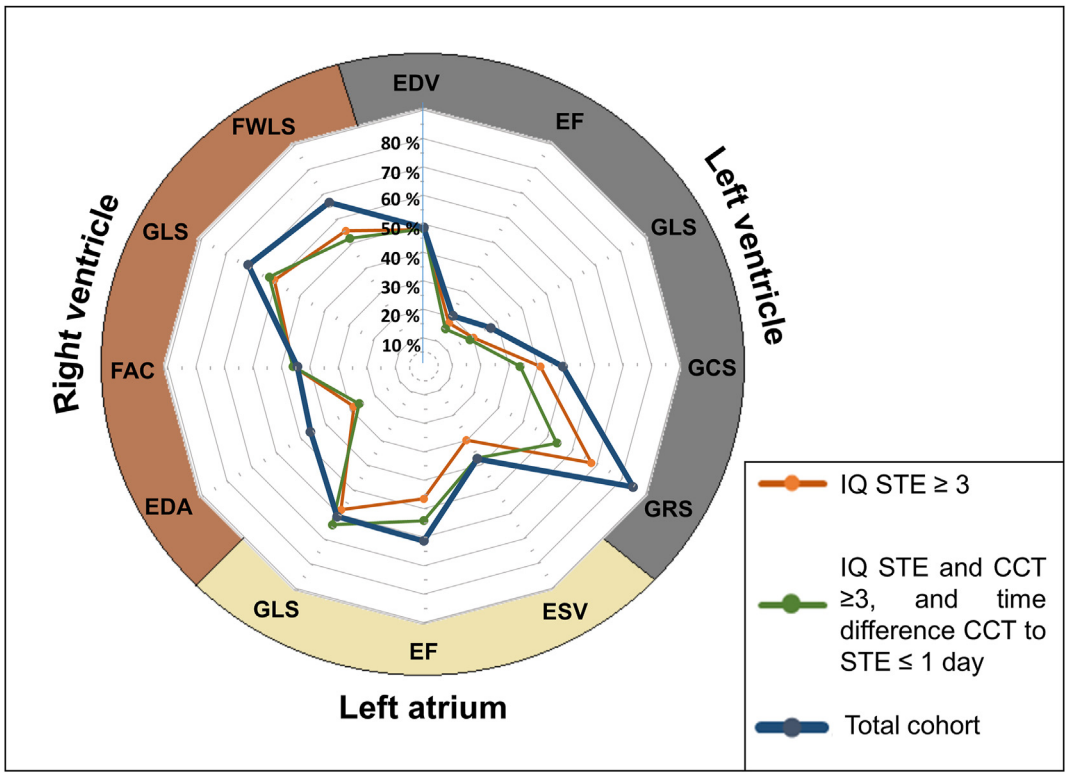

Fig. 6. Spiderplotted relative mean deviation between CCT and STE measurements in different subgroups. Abbreviations: CCT – 4D cardiac computed tomography, EDV/A – end diastolic volume/area, EF – ejection fraction, ESV/A – end systolic volume/area, FAC – fractional area change, FWLS – free wall longitudinal strain, GCS – global circumferential strain, GLS – global longitudinal strain, GRS – global radial strain.

depending on the time delay between CCT and STE. A relevant number of patients was excluded from analysis due to lacking or incomplete CCT or STE, which might result in selection bias. Calculation methods, workstations and vendors for imaging- and strain-acquisition varied between modalities. CCT strain was determined by feature tracking while echocardiography was analyzed by speckle tracking and we cannot exclude a systematic bias resulting from varying algorithm results specific for the used applications. Neither CCT-, nor STE image acquisition were dedicatedly performed for strain analysis but in clinical routine following standardized protocols. Instructed investigators and experts in echocardiography might provide images of better quality that are more feasible for strain analysis. Hence, this study might underestimate reproducibility of both modalities and particularly of echocardiographic assessments.

6. Conclusion

4D CCT feature tracking represents a reproducible method to assess left- and right ventricular and left atrial myocardial strain. Whereas agreement between modalities was strong for left ventricular global longitudinal strain, only moderate to poor correlation was depicted in right ventricular and left atrial strain, the latter possibly related to limited reproducibility in echocardiography.

Funding

None.

Declaration of competing interest

No specific funding was obtained for this work. The study was approved by the local ethics committee and was conducted in accordance with the Declaration of Helsinki. All patients provided written informed consent. The paper is not under consideration elsewhere, nor has the paper's contents been previously published. All authors have significantly contributed to the study and have the following disclosures: Dr. Okuno receives speaker fees from Abbott. Dr. Huber has received research grants from the Swiss National Science Foundation, the Helmut-Hartweg Foundation and the Foundation to Fight against Cancer, all for work outside the submitted study. Dr. Stortecky is the recipient of research grants to the institution from Edwards Lifesciences, Medtronic, Abbott Vascular and Boston Scientific, is a consultant for BTG and Teleflex and has received speaker fees from Boston Scientific. Dr. Windecker has received research grants to his institution from Abbott, Amgen, Boston, Biotronik, and St. Jude Medical, he has received no speaker fee. Dr. Pilgrim has received research grants to his institution from Edwards Lifesciences, Symetis, and Biotronik; has received speaker fees from Boston Scientific; and has received reimbursement for travel expenses from St. Jude Medical. Dr. Gräni received research funding from Swiss National Science Foundation and Innosuisse outside of the submitted work. Further Dr. Gräni received travel fees from Amgen and Bayer. All other authors report no conflicts.

Appendix A. Supplementary data

Supplementary data to this article can be found online at https://doi.org/10.1016/j.jcct.2022.01.003.

References

1. Voigt JU, Pedrizzetti G, Lysyansky P, et al. Definitions for a common standard for 2D speckle tracking echocardiography: consensus document of the EACVI/ASE/Industry Task Force to standardize deformation imaging. *J Am Soc Echocardiogr*. 2015;28:183–193. official publication of the American Society of Echocardiography.
2. Geyer H, Caracciolo G, Abe H, et al. Assessment of myocardial mechanics using speckle tracking echocardiography: fundamentals and clinical applications. official publication of the American Society of Echocardiography *J Am Soc Echocardiogr*. 2010;23:351–369. quiz 453-355.
3. Kalam K, Otahal P, Marwick TH. Prognostic implications of global LV dysfunction: a systematic review and meta-analysis of global longitudinal strain and ejection fraction. *Heart*. 2014;100:1673–1680.

4. Shen MT, Yang ZG, Diao KY, et al. Left ventricular involvement in arrhythmogenic right ventricular dysplasia/cardiomyopathy predicts adverse clinical outcomes: a cardiovascular magnetic resonance feature tracking study. *Sci Rep*. 2019;9:14235.
5. Florescu M, Magda LS, Enescu OA, Jinga D, Vinereanu D. Early detection of epirubicin-induced cardiotoxicity in patients with breast cancer. *J Am Soc Echocardiogr*. 2014;27:83–92. official publication of the American Society of Echocardiography.
6. Cho GY, Marwick TH, Kim HS, Kim MK, Hong KS, Oh DJ. Global 2-dimensional strain as a new prognosticator in patients with heart failure. *J Am Coll Cardiol*. 2009;54:618–624.
7. Amzulescu MS, De Craene M, Langet H, et al. Myocardial strain imaging: review of general principles, validation, and sources of discrepancies. *Eur Heart J Cardiovasc Imaging*. 2019;20:605–619.
8. Sengeløv M, Jørgensen PG, Jensen JS, et al. Global longitudinal strain is a superior predictor of all-cause mortality in heart failure with reduced ejection fraction. *JACC. Cardiovasc Imaging*. 2015;8:1351–1359.
9. Park JJ, Park JB, Park JH, Cho GY. Global longitudinal strain to predict mortality in patients with acute heart failure. *J Am Coll Cardiol*. 2018;71:1947–1957.
10. Lai W, Jie H, Jian-Xun D, et al. Impact of concomitant impairments of the left and right ventricular myocardial strain on the prognoses of patients with ST-elevation myocardial infarction. *Front cardiovasc med*. 2021;8:659364.
11. Fischer K, Obrist SJ, Erne SA, et al. Feature tracking myocardial strain incrementally improves prognostication in myocarditis beyond traditional CMR imaging features. *JACC. Cardiovasc Imaging*. 2020;13:1891–1901.
12. Schmid J, Kamml C, Zweiker D, et al. Cardiac magnetic resonance imaging right ventricular longitudinal strain predicts mortality in patients undergoing TAVI. *Front cardiovasc med*. 2021;8:644500.
13. Canessa M, Thamman R, Americo C, Soca G, Dayan V. Global longitudinal strain predicts survival and left ventricular function after mitral valve surgery: a meta-analysis. *Semin Thorac Cardiovasc Surg*. 2021;33:337–342.
14. Alashi A, Khullar T, Mentias A, et al. Long-term outcomes after aortic valve surgery in patients with asymptomatic chronic aortic regurgitation and preserved LVEF: impact of baseline and follow-up global longitudinal strain. *JACC. Cardiovasc Imaging*. 2020;13:12–21.
15. Ng ACT, Prihadi EA, Antoni ML, et al. Left ventricular global longitudinal strain is predictive of all-cause mortality independent of aortic stenosis severity and ejection fraction. *Eur Heart J Cardiovasc Imaging*. 2017;19:859–867.
16. Rowin EJ, Maron BJ, Wells S, et al. Usefulness of global longitudinal strain to predict heart failure progression in patients with nonobstructive hypertrophic cardiomyopathy. *Am J Cardiol*. 2021;151:86–92.
17. Lee Chuy K, Drill E, Yang JC, et al. Incremental value of global longitudinal strain for predicting survival in patients with advanced AL amyloidosis. *JACC Cardiovasc Oncol*. 2020;2:223–231.
18. Dons M, Jensen JS, Olsen FJ, et al. Global longitudinal strain corrected by RR-interval is a superior echocardiographic predictor of outcome in patients with atrial fibrillation. *Int J Cardiol*. 2018;263:42–47.
19. Hor KN, Baumann R, Pedrizzetti G, et al. Magnetic resonance derived myocardial strain assessment using feature tracking. *JoVE*. 2011:2356.
20. Kempny A, Fernández-Jiménez R, Orwat S, et al. Quantification of biventricular myocardial function using cardiac magnetic resonance feature tracking, endocardial border delineation and echocardiographic speckle tracking in patients with repaired tetralogy of fallot and healthy controls. *J Cardiovasc Magn Reson*. 2012;14:32.
21. Otto CM, Nishimura RA, Bonow RO, et al. 2020 ACC/AHA guideline for the management of patients with valvular heart disease: a report of the American college of cardiology/American heart association joint committee on clinical practice guidelines. *J Am Coll Cardiol*. 2020;77(4):450–500.
22. Okuno T, Corpataux N, Spano G, et al. True-severe stenosis in paradoxical low-flow low-gradient aortic stenosis: outcomes after transcatheter aortic valve replacement. *Eur Heart J Qual Care Clin Outcomes*. 2021;7(4):366–377.
23. Mitchell C, Rahko PS, Blauwet LA, et al. Guidelines for performing a comprehensive transthoracic echocardiographic examination in adults: recommendations from the American society of echocardiography. *J Am Soc Echocardiogr*. 2019;32:1–64. official publication of the American Society of Echocardiography.
24. Koo TK, Li MY. A guideline of selecting and reporting intraclass correlation coefficients for reliability research. *J Chiropr Med*. 2016;15:155–163.
25. Schober P, Boer C, Schwarte LA. Correlation coefficients: appropriate use and interpretation. *Anesth Analg*. 2018;126.
26. Sugimoto T, Dulgheru R, Bernard A, et al. Echocardiographic reference ranges for normal left ventricular 2D strain: results from the EACVI NORRE study. *Eur Heart J Cardiovasc Imaging*. 2017;18:833–840.
27. Chan J, Shiino K, Obonyo NG, et al. Left ventricular global strain analysis by two-dimensional speckle-tracking echocardiography: the learning curve. *J Am Soc Echocardiogr*. 2017;30:1081–1090. official publication of the American Society of Echocardiography.
28. Buss SJ, Schulz F, Mereles D, et al. Quantitative analysis of left ventricular strain using cardiac computed tomography. *Eur J Radiol*. 2014;83:e123–e130.
29. Pedrizzetti G, Claus P, Kilner PJ, Nagel E. Principles of cardiovascular magnetic resonance feature tracking and echocardiographic speckle tracking for informed clinical use. *J Cardiovasc Magn Reson*. 2016;18:51.
30. Langeland S, Wouters PF, Claus P, et al. Experimental assessment of a new research tool for the estimation of two-dimensional myocardial strain. *Ultrasound Med Biol*. 2006;32:1509–1513.
31. Luis SA, Yamada A, Khandheria BK, et al. Use of three-dimensional speckle-tracking echocardiography for quantitative assessment of global left ventricular function: a comparative study to three-dimensional echocardiography. *J Am Soc Echocardiogr*. 2014;27:285–291. official publication of the American Society of Echocardiography.
32. Obokata M, Nagata Y, Wu VC, et al. Direct comparison of cardiac magnetic resonance feature tracking and 2D/3D echocardiography speckle tracking for evaluation of global left ventricular strain. *Eur Heart J Cardiovasc Imaging*. 2016;17:525–532.
33. Venkatachalam S, Wu G, Ahmad M. Echocardiographic assessment of the right ventricle in the current era: application in clinical practice. *Echocardiography*. 2017;34:1930–1947.
34. Ammon F, Bittner D, Hell M, et al. CT-derived left ventricular global strain: a head-to-head comparison with speckle tracking echocardiography. *Int J Cardiovasc Imag*. 2019;35:1701–1707.
35. Szilveszter B, Nagy AI, Vattay B, et al. Left ventricular and atrial strain imaging with cardiac computed tomography: validation against echocardiography. *J Cardiovasc Comput Tomogr*. 2020;14:363–369.
36. Marwan M, Ammon F, Bittner D, et al. CT-derived left ventricular global strain in aortic valve stenosis patients: a comparative analysis pre and post transcatheter aortic valve implantation. *J Cardiovasc Comput Tomogr*. 2018;12:240–244.
37. Gegenava T, van der Bijl P, Hirasawa K, et al. Feature tracking computed tomography-derived left ventricular global longitudinal strain in patients with aortic stenosis: a comparative analysis with echocardiographic measurements. *J Cardiovasc Comput Tomogr*. 2020;14:240–245.
38. Claus P, Omar AMS, Pedrizzetti G, Sengupta PP, Nagel E. Tissue tracking technology for assessing cardiac mechanics: principles, normal values, and clinical applications. *JACC. Cardiovasc Imaging*. 2015;8:1444–1460.
39. Miskinyte E, Bucius P, Erley J, et al. Assessment of global longitudinal and circumferential strain using computed tomography feature tracking: intra-individual comparison with CMR feature tracking and myocardial tagging in patients with severe aortic stenosis. *J Clin Med*. 2019;8:1423.
40. Gegenava T, van der Bijl P, Vollema EM, et al. Prognostic influence of feature tracking multidetector row computed tomography-derived left ventricular global longitudinal strain in patients with aortic stenosis treated with transcatheter aortic valve implantation. *Am J Cardiol*. 2020;125:948–955.
41. Fukui M, Xu J, Thoma F, et al. Baseline global longitudinal strain by computed tomography is associated with post transcatheter aortic valve replacement outcomes. *J Cardiovasc Comput Tomogr*. 2020;14:233–239.
42. Tavakoli V, Sahba N. Cardiac motion and strain detection using 4D CT images: comparison with tagged MRI, and echocardiography. *Int J Cardiovasc Imag*. 2014;30:175–184.
43. Yotti R, Bermejo J, Benito Y, et al. Validation of noninvasive indices of global systolic function in patients with normal and abnormal loading conditions: a simultaneous echocardiography pressure-volume catheterization study. *Circ Cardiovasc imaging*. 2014;7:164–172.